SATURN'S MYSTERIOUS ARC-EMBEDDED MOONS: RECYCLED FLUFF? P. C. Thomas[1], J. A. Burns,[1] M. S. Tiscareno[1], M. M. Hedman[1], P. Helfenstein[1]. [1]Center for Radiophysics and Space Research, Cornell University, Ithaca, NY 14853 USA.

**Introduction:** The satellites of Saturn less than 150 km radius occupy several dynamical niches: within rings (Pan, Daphnis, Atlas, Prometheus, Pandora), Co-orbiting (Janus and Epimetheus), orbiting among faint rings or in ring arcs (Aegaeon, Methone, Anthe, Pallene) [1], and populating libration regions of larger moons (Telesto, Calypso, Polydeuces, and Helene). Hyperion orbits between Titan and Iapetus, and Phoebe is in a retrograde orbit well outside the orbits of the large satellites along with many other irregular satellites. The inner satellites groups are morphologically distinct from one another. All are low density: those for which masses and sizes have been well measured [2,3], have mean densities ρ of ~430-640 kg $m^{-3}$.

Cassini images of the arc-embedded moons show these are far smoother and more ovoid than other small satellites, whether of Saturn or other planets (and compared to small asteroids and comets) (Fig. 1). Methone and Pallene have been imaged well enough to use standard limb-finding and ellipsoidal solutions (54 and 14 pixels/mean radius); Aegaeon is less well measured (3 pixels/radius); fit ellipsoid shapes are given in Table 1. Methone is particularly smooth; the best images have 27 m/pixel and still show no surface or limb topography.

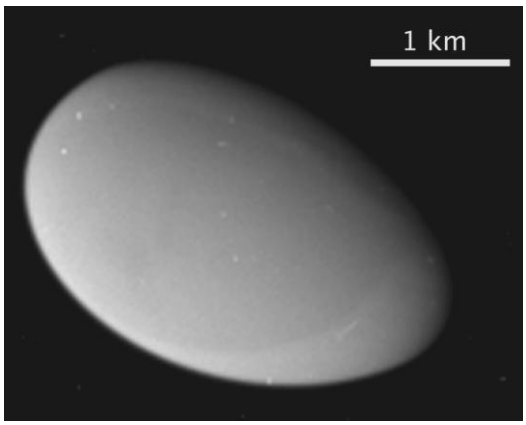


Fig. 1.Methone: image N1716192103, phase angle 63°. Spots are not reproduced image to image.

Table 1.
Ellipsoidal fits of shapes of embedded moons

| | a | b | c | km | | ± |
|---|---|---|---|---|---|---|
| Aegaeon | 0.70 | 0.25 | 0.20 | 0.05 | 0.06 | 0.08 |
| Methone | 1.94 | 1.29 | 1.21 | 0.02 | 0.04 | 0.02 |
| Pallene | 2.88 | 2.08 | 1.84 | 0.07 | 0.07 | 0.07 |

**Inferred densities:** The smoothness and excellent ellipsoidal fits suggest these objects have likely developed shapes close to equipotential surfaces. If so, the shapes may be used to infer mean densities. We model the surface accelerations and potential as a function of mean density (methods in [4]) to find the mean density that gives the smallest range of effective gravitational heights over the surface (dynamic heights; [5]). The results are shown in Table 2. Aegaeon's measurements and inferred properties are by far the least certain. Note that the equilibrium shapes for rapidly rotating, low-density objects are more prolate than the familiar (b-c)/(a-c)= 0.25; these objects have ratios closer to 0.1.

Accepting the assumptions, these satellites are very low density objects, but are in the range of densities inferred for some comet nuclei [6]. Any concentration of mass in "cores" would decrease the calculated mean density, and also would imply a mantle of even lower density [7]. Methone thus most likely has material in much of its body with ρ less than 360 kg $m^{-3}$.

Table 2. Inferred mean densities of embedded moons

| | density kg $m^{-3}$ | |
|---|---|---|
| Aegaeon | 540 | +160/-130 |
| Methone | 310 | +50/-30 |
| Pallene | 250 | +90/-60 |

**Discussion** Why are these objects different from other small Saturn satellites? Being embedded in ring arcs suggests a cycling of material to and from the arc that might smooth the surface. However, the optical depths of the arcs are sufficiently low and velocity of the moons relative to the arcs low enough that coating of one particle depth, be it 1 μm to 1 mm (with varying effective optical depths) implies resurfacing rates of order 1 m/$10^{10}$ y, far too low to compete with cratering processes [8]. The low density material may respond to hypervelocity impacts in a way that will smooth the objects more rapidly than on denser, higher gravity objects. Additionally, "exotic" processes such as electrostatic effects [9] might mobilize regolith in these very low g environments (Methone ~0.008 – 0.013 cm $s^{-2}$ surface gravity).

The puzzle of the geological smoothing is accompanied by the puzzle of a sharply-bounded, leading side darker albedo marking (Fig. 2, left). This area, exactly centered on the leading point, is ~13% darker than the rest (visible) of Methone where the albedo is ~0.70. UV/IR ratios show no statistically significant

trend with albedo (Fig. 2, right). The absence of correlated patterns of color and albedo on Methone suggests that the distinct albedo pattern is not the result of systematic variations in surface composition. Rather, the patterns may arise from variations in some other surface physical property, such as regolith grain size, soil compaction, or variations in particle microstructure. The albedo pattern may be especially conspicuous on Methone because of its remarkable smoothness. It is not yet known if similar patterns exist on the other arc-embedded satellites or the extent to which the pattern might exist but be obscured by surface relief on more heavily cratered small satellites. However, the geography of the albedo pattern is reminiscient of leading-side thermal anomalies that have been recently identified on Mimas and Tethys [10]. The anomalies are believed to be produced by preferential bombardment of high-energy electrons on the leading sides of those bodies. However, in those examples, the thermal anomalies coincide with a distinct increase in UV/IR coloration, which is either highly subdued or is not detectable in our ISS high-resolution coverage of Methone.

While the arc-embedded moons may approximate fluid behavior on geological timescales, it is not clear if this behavior is a function of size, orbital position, history, or materials. Further comparison of the distinct morphologies and photometry of the small satellites in the different dynamical niches may help elucidate the different modification processes and histories involved.

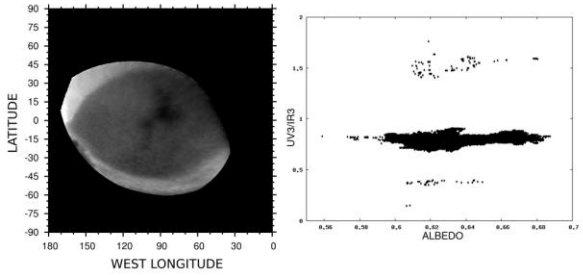


**Fig. 2: (Left)** Broadband visible wavelength (611nm) albedo map from the May 2012 Cassini flyby. A separate Minnaert photometric correction was applied to each image for normalizing pixel-by-pixel values of albedo at a reference incidence angle of 0° and phase angle of 5°. All of the images were projected to simple-cylindrical map coordinates before merging. Contrast-stretched to show subtle details. The prominent oval shaped dark region has a mean albedo of 0.61±0.06, including the dark feathery feature near the center that has values as low as 0.58. The bright material surrounding the oval albedo boundary has a mean normal albedo of 0.70±0.03. (Right) (CL1:UV3)/(CL1:IR3) ratio as a function of albedo from two Minnaert-corrected NAC images; N1716192136 (338nm) and N1716192257 (930nm).

**References:** [1] Hedman, M.M., et. al. (2009) *Icarus 199*, 378-386. [2] Jacobson, R.A., et al. (2008) *Astronomical Journal 135*, 261-263. [3] Porco, C. C.,et al., (2007) *Science 318*, 1602. [4] Thomas, P. C., (1993 *Icarus 105*, 326-334., [5] Vanicek, P., Krakiwsky, E.J., (1986) *Geodesy: The Concepts (2nd ed.) Elsevier, New York.*, [6] Richardson, J. E. et al. (2007) *Icarus 190*, 357-390. [7] Dermott, S.F. (1979) *Icarus 37*, 575–586., [8] Dones, L., et al. (2009) In *Saturn from Cassini-Huygens*. pp. 613–635, Springer. [9] Hirata, N., Miyamoto, H. (2012) *Icarus 220*, 106-113. [10] Howett, C. et al. (2012) *Icarus 221*, 1084-1088.

**Acknowledgements:** Supported in part by the Cassini project.